

BULLETIN

DE LA SOCIÉTÉ DES SCIENCES ET DES LETTRES DE ŁÓDŹ

2018

Vol. LXVIII

Recherches sur les déformations

no. 3

pp. 93–112

*Dedicated to the memory of
Professor Yurii B. Zelinskii*

Stanisław Bednarek and Julian Płoszajski

THE MAGNETIC FIELD PRODUCED BY A PROTONS BEAM WITH THE THREE-AXIAL GAUSS DISTRIBUTION

Summary

This paper contains a description of an original calculations method of electric field intensity and magnetic field induction which were produced by bunches assembling relativistic proton beams. The spatial distribution of electric charge density inside the bunch is described by the three-axial Gauss distribution. The method consists of component calculations of the electric field intensity at the frame of reference moving with the bunch and further, on the application of the Lorentz transformation to electromagnetic fields. As a result, we obtained values of components of electric field intensity and magnetic field induction at the rest frame of reference where could be located examined samples. Formula worked out with the method were discussed and gathered at the tables. Formula were applied to calculations of proton bunches accelerated in the LHC. The collected results were presented in the form of charts and discussed. Useful values of magnetic field induction and electric field intensity were very close to already published at the paper in which one-axial Gauss distribution was applied. The results contained in this paper confirmed possibility of using such particle bunches as sources of strong magnetic field pulses, useful among the others, in solid state physics, condensed phase physics and electronics as well.

Keywords and phrases: magnetic field, electric field, space distribution, Lorentz transformation, protons bunch, accelerator

1. Introduction

The aim of the research described in this paper were calculations of electric field intensity and magnetic field induction components values, produced by the relativistic particle beam the charge density of which inside the bunch is described by the three-axial Gauss distribution [1–3]. Results of these calculations have essential meaning for possible applications of such source of strong magnetic field pulses used in solid state physics, condensed phase physics and electronics, as well. The paper charge density distribution considered as part of this paper constitutes a more general case of one in a formerly published paper [4]. This case is more proper for a real application we meet in accelerators or accumulation rings [5–7]. Aim of this research was a more thorough analysis of produced fields and evaluation of their practical applications [8]. The method of calculations is similar to the formerly published paper [4]. Initially, the electric field intensity was calculated at the frame of reference moving with the bunch. Next, the Lorentz transformation was applied and values of components of the electric field intensity and magnetic field induction were calculated at the frame of reference connected with the sample.

2. Method of calculations

Let assume an orthogonal coordinate system $Oxyz$ connected to the bunch as in (Fig. 1). Let the origin of this coordinate system overlap at the middle of the bunch and the Ox axis was parallel to velocity of the bunch v (Fig. 1). At any point A (x_1, y_1, z_1) occurring inside of the bunch, quantity of particles $n(x_1, y_1, z_1)$ was expressed by the formula

$$n(x_1, y_1, z_1) = \frac{n_1}{\sigma_x \sigma_y \sigma_z (\sqrt{2\pi})^3} \exp \left[- \left(\frac{x_1^2}{2\sigma_x^2} + \frac{y_1^2}{2\sigma_y^2} + \frac{z_1^2}{2\sigma_z^2} \right) \right], \quad (1)$$

where n_1 – the whole quantity of particles in the bunch, $\sigma_x \sigma_y \sigma_z$ – standard deviations.

An element of the charge dq occurring inside any surrounding of point A could be calculated by the formula

$$dq = n(x_1, y_1, z_1) e dx_1 dy_1 dz_1. \quad (2)$$

where e meant the charge of one particle (this was typically an elementary charge).

In order to calculate the value of an element of the electric field intensity dE , produced at any point B (x_2, y_2, z_2) by the charge element dq we used well-known electrostatics formula [9]

$$dE = \frac{1}{4\pi\epsilon_0} \frac{dq}{r^2}, \quad (3)$$

where ϵ_0 represents the electrical permittivity of free space.

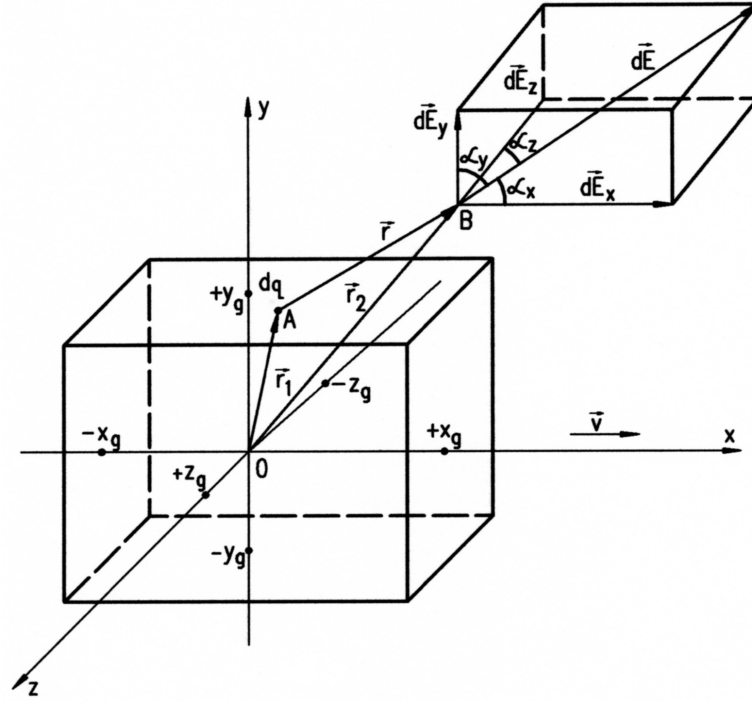


Fig. 1. Frame of reference connected to the bunch of particles and accepted for calculations; 0 – bunch middle, B – point chosen for field intensity calculations, dq – charge element, $\mathbf{r}_1, \mathbf{r}_2, \mathbf{r}$ – position vectors respectively of: charge element and point B relatively to the bunch middle and point B relatively to charge element, $d\mathbf{E}_x, d\mathbf{E}_y, d\mathbf{E}_z, d\mathbf{E}$ – components of electric field intensity and the net element, $\pm x_g, \pm y_g, \pm z_g$ – conventional bunch boundary, \mathbf{v} – bunch velocity.

The distance r between points A and B which was a part of formula (3) was calculated by means of the Pythagorean theorem

$$r = \sqrt{(x_2 - x_1)^2 + (y_2 - y_1)^2 + (z_2 - z_1)^2}. \quad (4)$$

Components of the elements of the electric field intensity dE_x, dE_y, dE_z , directed into $0x, 0y, 0z$ axes were described by the formulae:

$$dE_x = dE \cos \alpha_x, \quad (5)$$

$$dE_y = dE \cos \alpha_y, \quad (6)$$

$$dE_z = dE \cos \alpha_z. \quad (7)$$

Direction cosines, found in formulae (5–7) were calculated by the formulae:

$$\cos \alpha_x = \frac{x_2 - x_1}{r}, \quad (8)$$

$$\cos \alpha_y = \frac{y_2 - y_1}{r}, \quad (9)$$

$$\cos \alpha_z = \frac{z_2 - z_1}{r}. \quad (10)$$

In order to calculate the components of electric field intensity E_x, E_y, E_z , in directions of $0x, 0y, 0z$ axes, should be integrated as expressed in formulae expressed by within the limits of the bunch volume, meaning the calculation of integrals (5–7):

$$E_x(x_2, y_2, z_2) = \int_{x_1=-x_g}^{x_1=+x_g} \int_{y_1=-y_g}^{y_1=+y_g} \int_{z_1=-z_g}^{z_1=+z_g} dE_x, \quad (11)$$

$$E_y(x_2, y_2, z_2) = \int_{x_1=-x_g}^{x_1=+x_g} \int_{y_1=-y_g}^{y_1=+y_g} \int_{z_1=-z_g}^{z_1=+z_g} dE_y, \quad (12)$$

$$E_z(x_2, y_2, z_2) = \int_{x_1=-x_g}^{x_1=+x_g} \int_{y_1=-y_g}^{y_1=+y_g} \int_{z_1=-z_g}^{z_1=+z_g} dE_z. \quad (13)$$

Formulae (5–7) were substituted suitably to (11–13) together with (8–10) and (3, 4, 2, 1). As the final result following formulae were received:

$$E_x(x_2, y_2, z_2) = \frac{e}{4\pi\epsilon_0} \times \quad (14)$$

$$\int_{x_1=-x_g}^{x_1=+x_g} \int_{y_1=-y_g}^{y_1=+y_g} \int_{z_1=-z_g}^{z_1=+z_g} \left\{ \frac{\frac{n_1}{\sigma_x \sigma_y \sigma_z (\sqrt{2\pi})^3} \exp\left[-\left(\frac{x_1^2}{2\sigma_x^2} + \frac{y_1^2}{2\sigma_y^2} + \frac{z_1^2}{2\sigma_z^2}\right)\right](x_2 - x_1)}{\sqrt{[(x_2 - x_1)^2 + (y_2 - y_1)^2 + (z_2 - z_1)^2]^3}} \right\} dx_1 dy_1 dz_1,$$

$$E_y(x_2, y_2, z_2) = \frac{e}{4\pi\epsilon_0} \times \quad (15)$$

$$\int_{x_1=-x_g}^{x_1=+x_g} \int_{y_1=-y_g}^{y_1=+y_g} \int_{z_1=-z_g}^{z_1=+z_g} \left\{ \frac{\frac{n_1}{\sigma_x \sigma_y \sigma_z (\sqrt{2\pi})^3} \exp\left[-\left(\frac{x_1^2}{2\sigma_x^2} + \frac{y_1^2}{2\sigma_y^2} + \frac{z_1^2}{2\sigma_z^2}\right)\right](y_2 - y_1)}{\sqrt{[(x_2 - x_1)^2 + (y_2 - y_1)^2 + (z_2 - z_1)^2]^3}} \right\} dx_1 dy_1 dz_1,$$

$$E_z(x_2, y_2, z_2) = \frac{e}{4\pi\epsilon_0} \times \quad (16)$$

$$\int_{x_1=-x_g}^{x_1=+x_g} \int_{y_1=-y_g}^{y_1=+y_g} \int_{z_1=-z_g}^{z_1=+z_g} \left\{ \frac{\frac{n_1}{\sigma_x \sigma_y \sigma_z (\sqrt{2\pi})^3} \exp\left[-\left(\frac{x_1^2}{2\sigma_x^2} + \frac{y_1^2}{2\sigma_y^2} + \frac{z_1^2}{2\sigma_z^2}\right)\right](z_2 - z_1)}{\sqrt{[(x_2 - x_1)^2 + (y_2 - y_1)^2 + (z_2 - z_1)^2]^3}} \right\} dx_1 dy_1 dz_1,$$

which allowed for the calculation of the components of electric field intensity E_x, E_y, E_z at the frame of reference $0xyz$ connected to the bunch.

In order to calculate the components values of electric field intensity E'_x, E'_y, E'_z and the components of magnetic field induction B'_x, B'_y, B'_z at the frame of reference $0x'y'z'$ connected to the sample, Lorentz transformation was applied, expressed by the following formulae [10]:

$$E'_x = E_x \quad E'_y = \gamma(E_y - vB_z) \quad E'_z = \gamma(E_z + vB_y), \quad (17)$$

$$B'_x = B_x \quad B'_y = \gamma\left(B_y + \frac{\beta}{c}E_z\right) \quad B'_z = \gamma\left(B_z - \frac{\beta}{c}E_y\right), \quad (18)$$

where

$$\beta = \frac{v}{c} \quad \text{and} \quad \gamma = \frac{1}{\sqrt{1 - \beta^2}}. \quad (19)$$

After substitution of values received from the formulae (14–16) into formulae (18, 19) we could calculate all components of electric field intensity and magnetic field induction at any point of volume of the examined sample. This procedure has been used to obtain results shown in further considerations. It is important to note that in accordance with the Lorentz transformation y, z , coordinates perpendicular to the direction of the bunch movement did not change after passage to frame of reference connected with the sample. Therefore this frame of reference has been marked as $0x'y'z'$, instead of $0x'y'z$.

3. Results of the calculations

Before providing detailed results of the calculations, it could be worthwhile to mention about some general features of electric and magnetic fields, which are produced by the bunch of particles of the considered charge distribution. Because the charge distribution at the bunch had neither a spherical nor a cylindrical symmetry, so all the components of electric field intensity at the frame of reference connected to the bunch expressed by the formulae (14–16), could be different from zero. Moreover, charges at the bunch were motionless with regard to this frame of reference. Therefore, all components of magnetic field induction were equal zero. After taking into account these conditions from the Lorentz transformation, expressed by the formulae (17, 18), the following formulae describing components of electric field intensity and magnetic field induction were worked out for the frame of reference connected to the sample. The formulae received in this way were shown as part of Tab. 1.

For the further analysis of the spatial distribution of electric and magnetic fields characteristic planes, lines and points in vicinity of the bunch were chosen, which were shown in Fig. 2. The considered bunch of particles with a three-dimensional Gauss distribution did not have cylindrical symmetry as it was analyzed, as the former paper with one-dimensional Gauss distribution, but had however three planes of symmetry $x0y$, $y0z$, and $z0x$ and three axes of symmetry $0x$, $0y$ and $0z$. Because

Table 1. Specification of formulae on components of electric field intensity and magnetic field induction at any point of frame $0xyz$ connected to the bunch of particles and the frame $0x'yz'$, which was connected to the sample.

	Components of electric field intensity	Components of magnetic field induction
Frame connected to the bunch	$E_x \neq 0$	$B_x = 0$
	$E_y \neq 0$	$B_y = 0$
	$E_z \neq 0$	$B_z = 0$
Frame connected to the sample	$E'_x = E_x$	$B'_x = 0$
	$E'_y = \gamma E_y$	$B'_y = \gamma \frac{\beta}{c} E_z$
	$E'_z = \gamma E_z$	$B'_z = -\gamma \frac{\beta}{c} E_y$

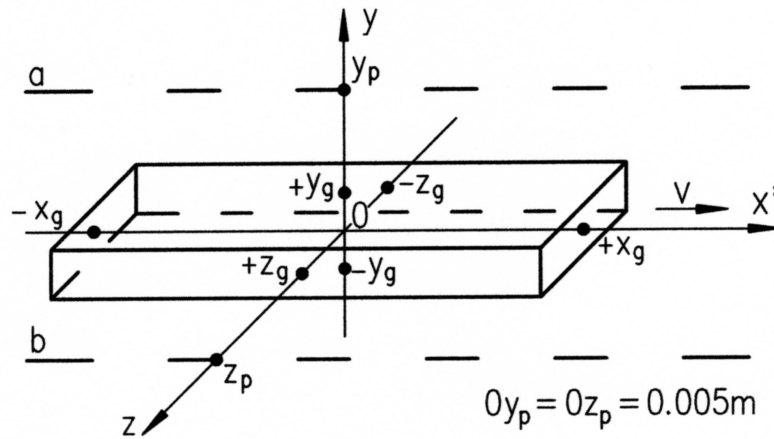


Fig. 2. Position of characteristic planes, lines and points in vicinity of the bunch of particles where components of electric and magnetic fields were analyzed; $\pm x_g, \pm y_g, \pm z_g$ – conventional bunch boundary, a, b – straight lines passing in distance of $y_p = z_p = 0.005$ m from the bunch axis, \mathbf{v} – bunch velocity.

of such symmetries, some components of the electric and magnetic fields have in those points values equal zero. Moreover, the conducted analysis two lines a, b , were distinguished, parallel to axis $0x$ (longitudinal to bunch axis) and passing at the distance of 0.005 m. Those lines were interesting from a practical standpoint of view because at this distance it was possible to place samples of the size of 1 mm. Moreover, such sample distance from the bunch axis was suggested in the previous article [4]. It will be possible thanks to the above suggestion, to conduct an appropriate comparison and discussion of the results.

In next step of the analysis the discussed earlier symmetries and assumptions are

considered. It enable to derive formulae to calculation of the electric and magnetic components at characteristics places. Mentioned places consist of the planes and axis of the frame connected to the particle bunch and the sample. The derived formulae are collected in Tables 2 and 3.

Table 2. Specification of formulae on components of electric field intensity at the characteristic places frame $0xyz$ connected to the particle bunch (all components of magnetic field induction at this frame of reference were zero).

Components of electric field intensity			
Plane $x0y$ $z = 0$	$E_x = E_x(x, y)$ $E_y = E_y(x, y)$ $E_z = E_z(x, y)$	axis $0x$ $y = 0$ $z = 0$	$E_x = E_x(x)$ $E_y = 0$ $E_z = 0$
		axis $0y$ $x = 0$ $z = 0$	$E_x = 0$ $E_y = E_y(y)$ $E_z = 0$
Plane $x0z$ $y = 0$	$E_x = E_x(x, z)$ $E_y = E_y(x, z)$ $E_z = E_z(x, z)$	axis $0x$ $y = 0$ $z = 0$	$E_x = E_x(x)$ $E_y = 0$ $E_z = 0$
		axis $0z$ $x = 0$ $y = 0$	$E_x = 0$ $E_y = 0$ $E_z = E_z(z)$
Plane $y0z$ $x = 0$	$E_x = E_x(y, z)$ $E_y = E_y(y, z)$ $E_z = E_z(y, z)$	axis $0y$ $x = 0$ $z = 0$	$E_x = 0$ $E_y = E_y(y)$ $E_z = 0$
		axis $0z$ $x = 0$ $y = 0$	$E_x = 0$ $E_y = 0$ $E_z = E_z(z)$

Next step of the research was based on calculation of the values of components of the electric field intensity and magnetic field induction at the frame $0x'yz$ connected to the sample as dependence from coordinates indicating point of location at this

Table 3. Specification of formulae on components of electric field intensity and magnetic field induction at characteristic places of frame $0x'y'z'$ connected to the sample.

Components of electric field intensity				Components of magnetic field induction			
Plane $x'0y'$ $z=0$	$E'_x = E_x(x', y)$ $E'_y = \gamma E_y(x', y)$ $E'_z = \gamma E_z(x', y)$	axis	$E'_x = E_x(x')$	Plane $x'0y'$ $z=0$	$B'_x = 0$ $B'_y = \gamma \frac{\beta}{c} E_z(x', y)$ $B'_z = -\gamma \frac{\beta}{c} E_y(x', y)$	axis	$B'_x = 0$
		$0x'$	$E'_y = 0$			$0x'$	$B'_y = 0$
		$y=0$	$E'_z = 0$			$y=0$	$B'_z = 0$
		$z=0$				$z=0$	
		axis	$E'_x = 0$			axis	$B'_x = 0$
		$0y'$	$E'_y = \gamma E_y(y)$			$0y'$	$B'_y = 0$
		$x'=0$	$E'_z = 0$			$x'=0$	$B'_z = -\gamma \frac{\beta}{c} E_y(y)$
		$z=0$				$z=0$	
Plane $x'0z'$ $y=0$	$E'_x = E_x(x', z)$ $E'_y = \gamma E_y(x', z)$ $E'_z = \gamma E_z(x', z)$	axis	$E'_x = E_x(x')$	Plane $x'0z'$ $y=0$	$B'_x = 0$ $B'_y = \gamma \frac{\beta}{c} E_z(x', z)$ $B'_z = -\gamma \frac{\beta}{c} E_y(x', z)$	axis	$B'_x = 0$
		$0x'$	$E'_y = 0$			$0x'$	$B'_y = 0$
		$y=0$	$E'_z = 0$			$y=0$	$B'_z = 0$
		$z=0$				$z=0$	
		axis	$E'_x = 0$			axis	$B'_x = 0$
		$0z'$	$E'_y = 0$			$0z'$	$B'_y = \gamma \frac{\beta}{c} E_z(z)$
		$x'=0$	$E'_z = \gamma E_z(z)$			$x'=0$	$B'_z = 0$
		$y=0$				$y=0$	
Plane $y'0z'$ $x'=0$	$E'_x = E_x(y, z)$ $E'_y = \gamma E_y(y, z)$ $E'_z = \gamma E_z(y, z)$	axis	$E'_x = 0$	Plane $y'0z'$ $x'=0$	$B'_x = 0$ $B'_y = \gamma \frac{\beta}{c} E_z(y, z)$ $B'_z = -\gamma \frac{\beta}{c} E_y(y, z)$	axis	$B'_x = 0$
		$0y'$	$E'_y = \gamma E_y(y)$			$0y'$	$B'_y = 0$
		$x'=0$	$E'_z = 0$			$x'=0$	$B'_z = -\gamma \frac{\beta}{c} E_y(y)$
		$z=0$				$z=0$	
		axis	$E'_x = 0$			axis	$B'_x = 0$
		$0y'$	$E'_y = 0$			$0y'$	$B'_y = \gamma \frac{\beta}{c} E_z(z)$
		$x'=0$	$E'_z = \gamma E_z(z)$			$x'=0$	$B'_z = 0$
		$z=0$				$z=0$	

Table 4. Specification of parameters of proton bunch in LHC accepted for calculations.

No.	Name of parameter	Sign	Value
1	Number of particles (protons) at bunch	n_1	$1.15 \cdot 10^{11}$
2	Size of bunch in $0x$ axis direction	x_g	3.775 cm
3	Size of bunch in $0y$ axis direction	y_g	16 μm
4	Size of bunch in $0z$ axis direction	z_g	70.9 μm
5	Energy of particles	E	7 TeV
6	Velocity of particles	v	0.999 999 991 c
7	Energy increase (Lorentz factor)	γ	$7.46 \cdot 10^3$

frame of reference. For these calculations, the same initial values were accepted as at the former publication and were supplemented with transversal dimensions of a focused bunch of protons in the LHC accelerator [11–14] as accessible in literature. The collected values were presented in Tab. 4. Knowing the bunch dimensions, standard deviations were calculated $\sigma_x, \sigma_y, \sigma_z$, which are in a three-axial Gauss distribution, expressed by formula (1). To do this, following formulae were applied:

$$x_g = \pm n\sigma_x, \quad (20)$$

$$y_g = \pm n\sigma_y, \quad (21)$$

$$z_g = \pm n\sigma_z, \quad (22)$$

where n is a natural number. $n = 3$ was accepted for the calculations, which allows to confirm, that volume limited to the size of bunch included 99,7% its total electric charge.

Charts received as the result of conducted calculations were shown in Fig. 3–22.

Due to the huge range of change of electric field intensity component values $E'y, E'z$, and magnetic field induction $B'y, B'z$ their relevant coordinates y , and z were divided into two sub ranges for which separate charts were generated. These included: range of small distances 0–200 μm , and medium distances 0–2 mm. Moreover, charts were presented for the whole range of coordinates taken into account as part of the calculations. Such a presentation allowed for a better preservation of the linear scale and better illustrates the character of the changes observed.

4. Discussion of the results

The calculations conducted showed that the sample located close to the bunch of particles which had three-axial Gauss distribution for charge density, will be subjected to pulses of both, magnetic and electric fields. A comparison of the Charts has

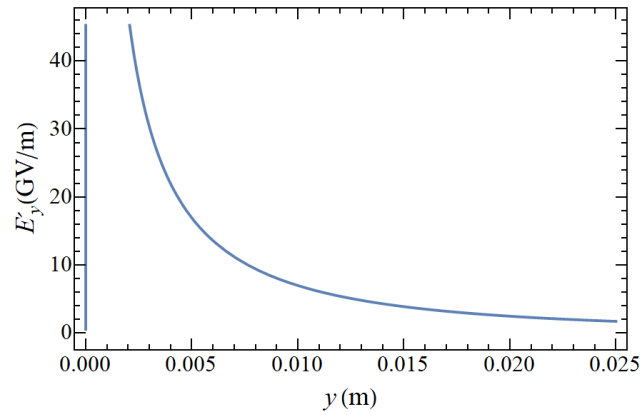


Fig. 3. Dependence of components electric field intensity E'_y , as a function of distance from the bunch axis measured by y in plane transversal symmetry to the bunch ($x'_0 = 0$) at frame of reference sample for the whole range of distance 0–25 mm.

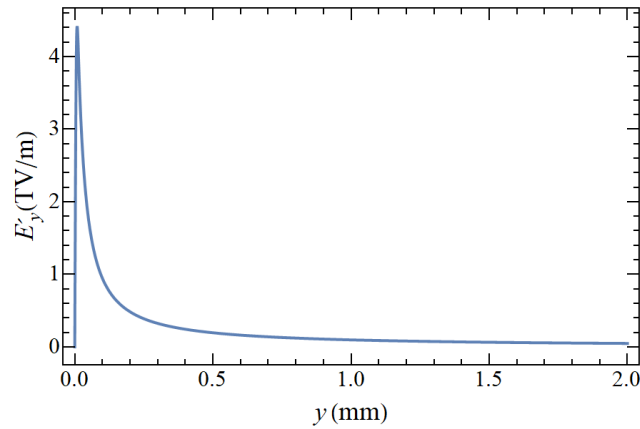


Fig. 4. Dependence of components electric field intensity E'_y , as a function of distance from the bunch axis measured by y in plane transversal symmetry to the bunch ($x'_0 = 0$) at sample frame of reference for the whole range of distance 0–2 mm.

been presented as Fig. 17 and 18 and in Fig. 9 and 10 as well, allowed to state that, the duration of field pulses was equal. A similar situation has been observed in case of bunch of particles having one-dimensional Gauss distribution of charge density, as considered in the previous paper. Due to the lack of rotational symmetry in the case of the three-dimensional Gauss distribution for charge density of a particle bunch, the sample could be subjected to more complex distributions based on a simultaneous occurrence of two mutually perpendicular three components of electric field intensity and two components of magnetic field induction.

The most important conclusion from conducted calculations is based on the fact that the values of the magnetic field induction and electric field intensity in the distance from the bunch axis, having practical meaning from the point of view of placing a sample with macroscopic size of 1 mm, are close to the ones obtained values as in the previous paper. This indicates the propriety of the conducted calculations

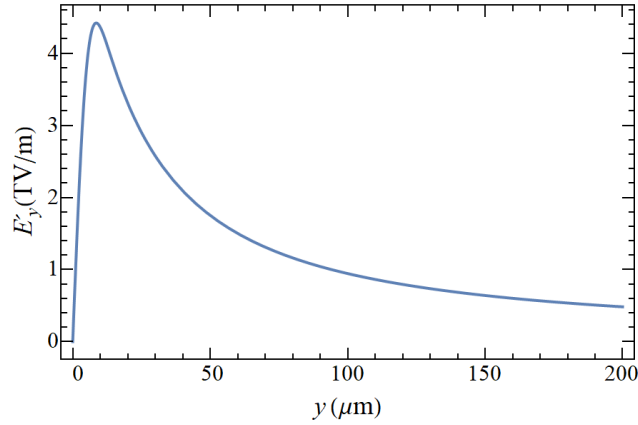


Fig. 5. Dependence of components electric field intensity E'_y , as a function of distance from the bunch axis measured by y in plane transversal symmetry to the bunch ($x'_0 = 0$) at sample frame of reference for the whole range of distance 0–200 μm .

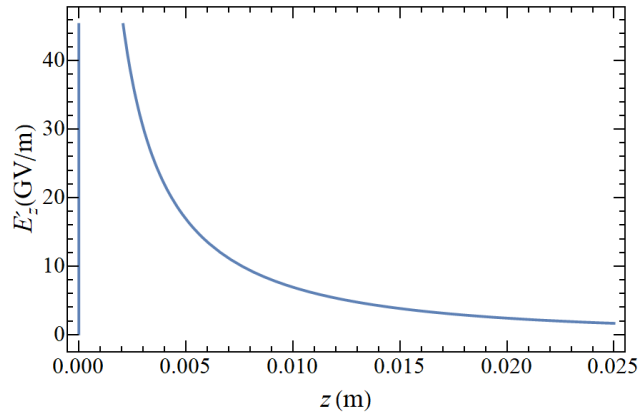


Fig. 6. Dependence of components electric field intensity E'_z , as a function of distance from the bunch axis measured by y in plane transversal symmetry to the bunch ($x'_0 = 0$) at sample frame of reference for the whole range of distance 0–25 mm.

and usefulness of the bunch model, in both, a one-dimensional and three-dimensional Gauss distributions. As an example, comparing Fig. 8 in the previous paper [4] and Fig. 17 included in this paper, it is apparent that maximal values of magnetic field induction were respectively 57 T and 56 T.

The application of the three-dimensional Gauss distribution for charge density allowed to show dependence of the electric field intensity and the magnetic field induction in an area very close to the bunch axis, i.e. inside of the bunch. Because the bunch did not have any sharply defined boundary the defining of the interior is purely theoretical in meaning. In case of a one-dimensional Gauss distribution, the interior of the bunch was not considered, because in accordance with this model of electric field intensity and magnetic field induction, the values have progressed in the direction of infinity, which did not of course make any physical sense (see Fig. 5 and

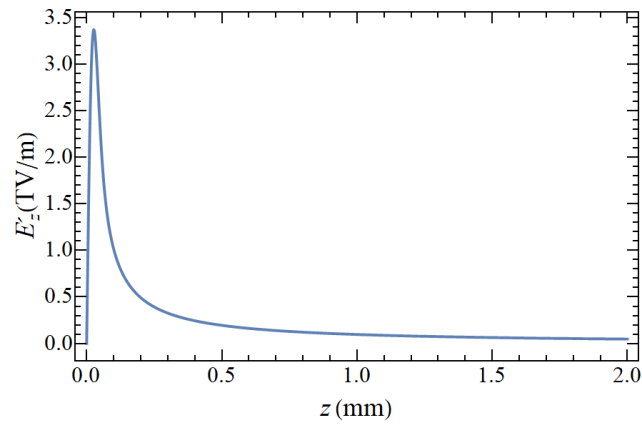


Fig. 7. Dependence of components of electric field intensity E'_z , as a function of distance from the bunch axis measured by y in plane transversal symmetry to the bunch ($x'_0 = 0$) at sample frame of reference for the whole range of distance 0–2 mm.

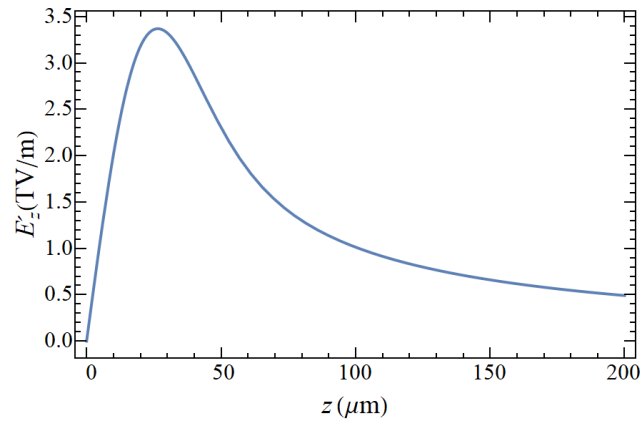


Fig. 8. Dependence of components electric field intensity E'_z , as a function of distance from the bunch axis measured by y in plane transversal symmetry to the bunch ($x'_0 = 0$) at sample frame of reference for the whole range of distance 0–200 μm .

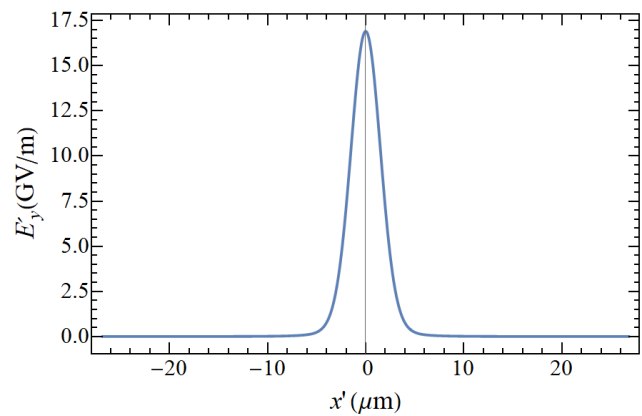


Fig. 9. Dependence of components electric field intensity E'_y , as a function of distance x'_0 from the transversal plain symmetry for booked distance from the bunch axis $y_p = 0.005$ m at the sample frame of reference.

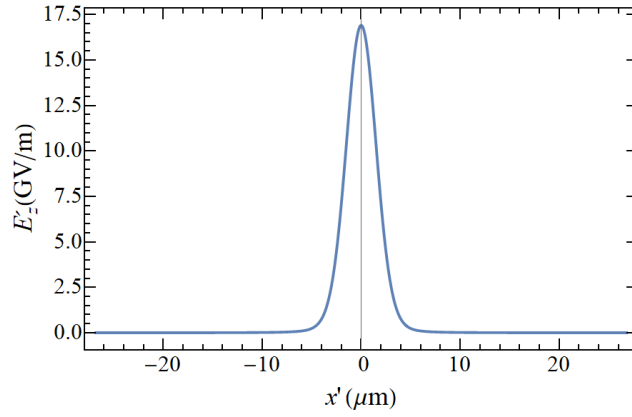


Fig. 10. Dependence of components of electric field intensity E'_z as a function of distance x'_0 from the transversal plain symmetry for established distance from the bunch axis $z_p = 0.005$ m at the sample frame of reference.

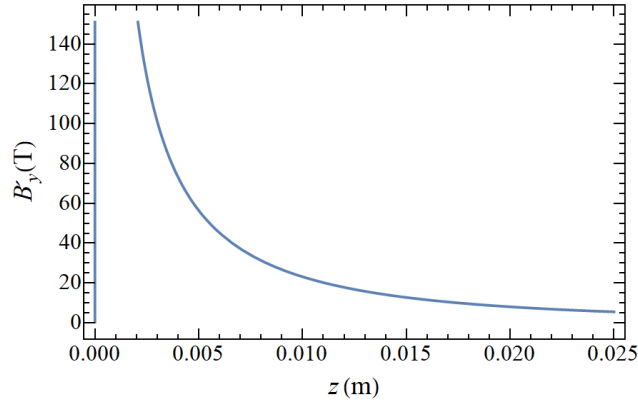


Fig. 11. Dependence of components of magnetic field induction B'_y , as a function of distance from the bunch axis measured with coordinate y in transversal plain of bunch symmetry ($x'_0 = 0$) at the sample frame of reference for the whole range of distances 0–25 mm.

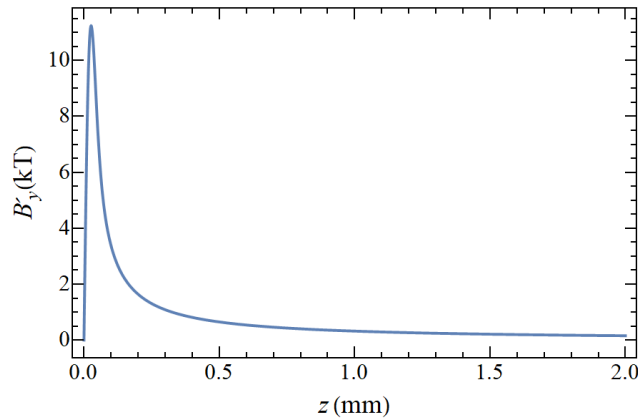


Fig. 12. Dependence of components of magnetic field induction B'_y , as a function of distance from the bunch axis measured with coordinate y in transversal plain of bunch symmetry ($x'_0 = 0$) at the sample frame of reference for the medium range of distances 0–2 mm.

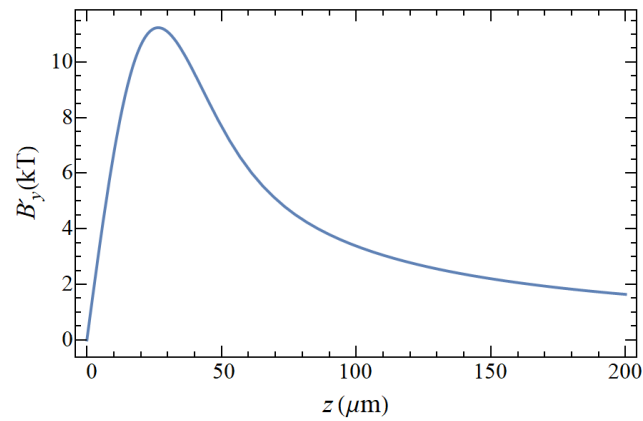


Fig. 13. Dependence of components of magnetic field induction B'_y , as a function of distance from the bunch axis measured with coordinate y in transversal plain of bunch symmetry ($x'_0 = 0$) at the sample frame of reference for the small range of distances 0–200 μm .

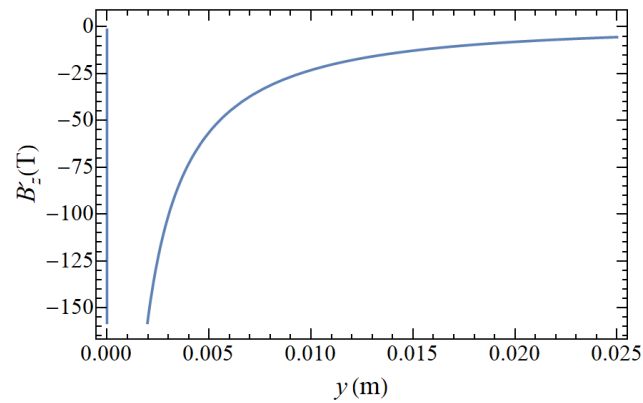


Fig. 14. Dependence of components magnetic field induction B'_z , as a function of distance from the bunch axis measured with coordinate y in transversal plain of bunch symmetry ($x'_0 = 0$) at the sample frame of reference for the whole range of distances 0–25 mm.

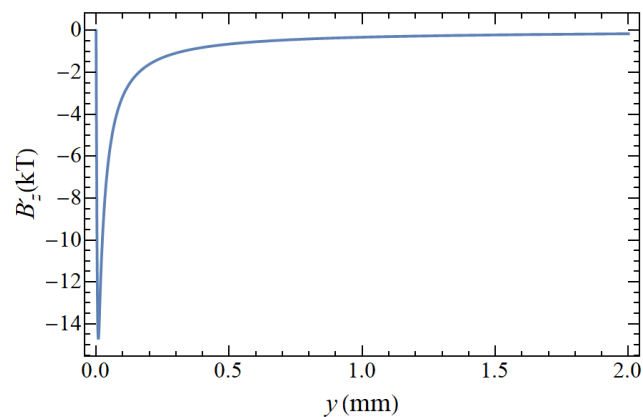


Fig. 15. Dependence of components of magnetic field induction B'_z , as a function of distance from the bunch axis measured with coordinate y in transversal plain of bunch symmetry ($x'_0 = 0$) at the sample frame of reference for the medium range of distances 0–2 mm.

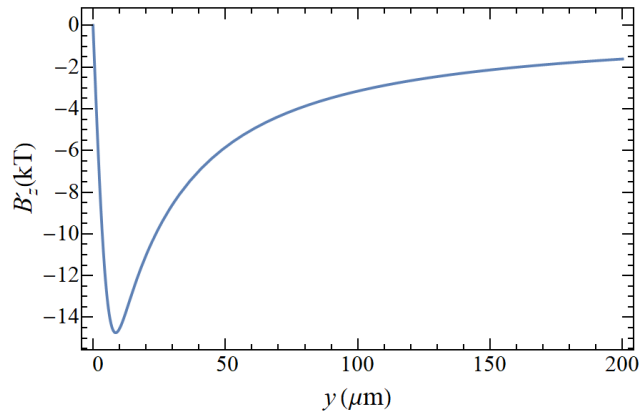


Fig. 16. Dependence of components of magnetic field induction B'_z , as a function of distance from the bunch axis measured with coordinate y in transversal plain of bunch symmetry ($x'_0 = 0$) at the sample frame of reference for the small range of distances 0–200 μm .

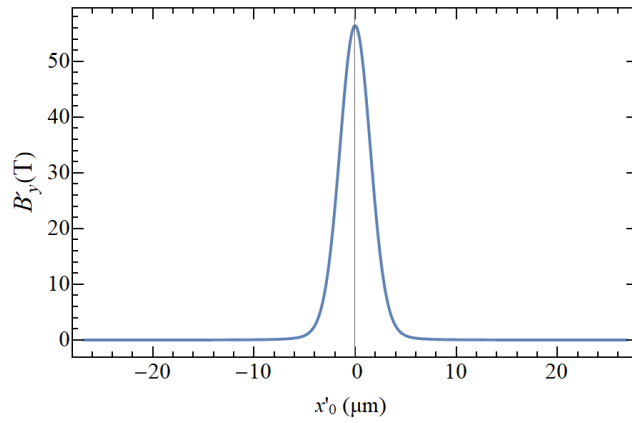


Fig. 17. Dependence of component of magnetic field induction B'_y , as a function of distance x'_0 from transversal plain bunch symmetry for booked distance from bunch axis $y_p = 0.005$ m in the frame of the sample.

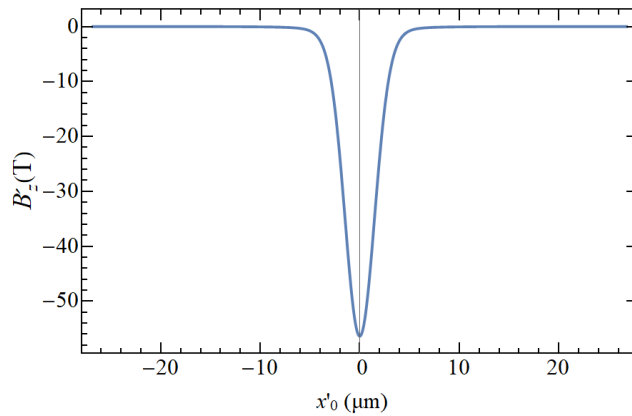


Fig. 18. Dependence of component of magnetic field induction B'_z , as a function of distance x'_0 from transversal plain bunch symmetry for booked distance from bunch axis $z_p = 0.005$ m in the frame of the sample.

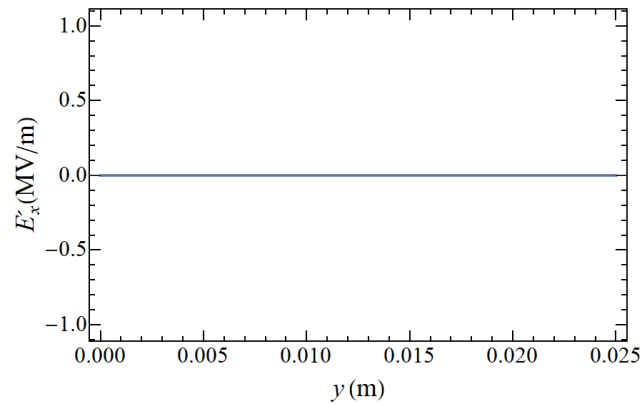


Fig. 19. Dependence of component of electric field intensity E'_x , as a function of coordinate y in transversal plain bunch symmetry ($x'_0 = 0$) in the frame of the sample.

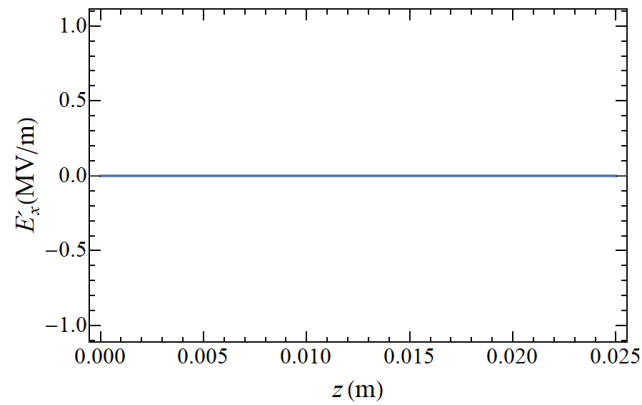


Fig. 20. Dependence of component of electric field intensity E'_x , as a function of distance x'_0 from transversal plain bunch symmetry for booked distance from bunch axis $y_p = 0.005$ m in the frame of the sample.

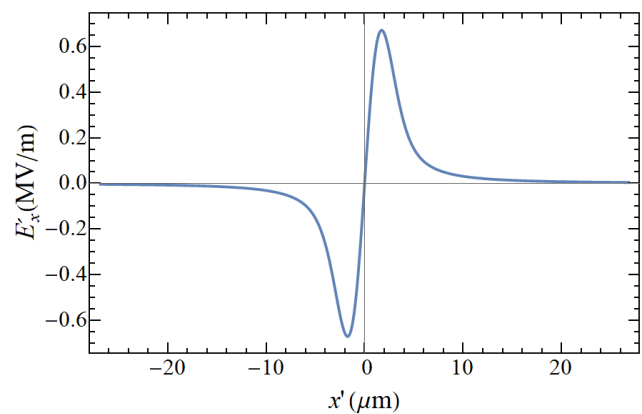


Fig. 21. Dependence of component of electric field intensity E'_x , as a function of coordinate z in transversal plain bunch symmetry ($x'_0 = 0$) in the frame of the sample.

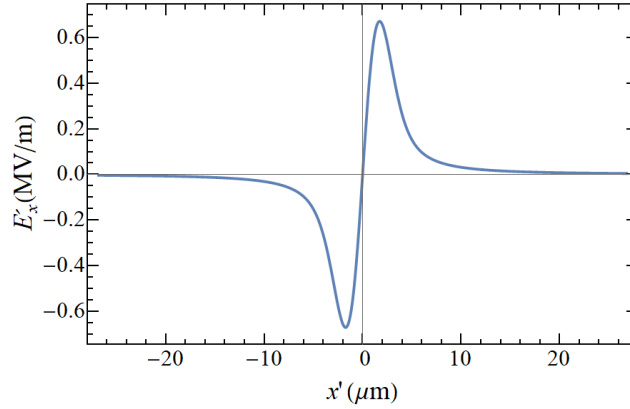


Fig. 22. Dependence of component of electric field intensity E'_x , as a function of distance x'_0 from transversal plain bunch symmetry for booked distance from bunch axis $z_p = 0.005$ m in the frame of the sample.

6 in paper [4]). In the case of a three-dimensional Gauss distribution, the electric field intensity and magnetic field induction values inside the bunch, grow from zero to certain maximal values which were reached close to the theoretical boundary of the bunch (see Fig. 4, 5 and 7, 8).

If the spatial distribution inside the bunch were homogenous, meaning that the charge density had a constant value and the bunch were infinitely long, than in accordance with the Gauss law and Ampere law, the dependence of electric field intensity and magnetic field induction inside the bunch, would be described by linear functions. Moreover, a homogenous charge distribution would have a sharp boundary outside which, the density value would be zero. On this boundary, values of the electric field intensity and magnetic field induction would reach their maximum after which the values would decrease in an inversely proportional manner to the distance from the bunch axis. These maximum values had first type discontinuities, which meant that the functions describing the dependencies of the electric field intensity and magnetic field induction could not be differentiable. Because charge density along the distance from the bunch axis changes in accordance with the Gauss distribution, then the increases of the electric field intensity and magnetic field induction are of nonlinear character. Moreover, these dependences did not have sharp boundary and curved sections describing the electric field intensity or magnetic field induction and passes smoothly into the section describing decrease of these values.

Interesting was also the fact that values of electric field intensity and magnetic field induction inside the bunch and close to its theoretical boundaries, reached very high values. They values are much greater than those found in many physical devices and phenomena observed on Earth. For instance, in accordance with Fig. 12 and 13 as well as 14 and 16, the magnetic field induction values B'_y, B'_z at the distances $8 \mu\text{m}$

from the bunch axis had respective values of 11.5 kT and 14.8 kT, and electric field intensity E'_y, E'_z achieved suitably 0.58 GV/m and 0.45 GV/m. For comparison, the magnetic field induction pulses produced by explosive compression of magnetic flux reach the magnitudes of 800–1000 T, while record values of induction achieved with this method equaled 2500 T [15, 16]. The highest values for magnetic field induction occurring in the focus a very strong laser pulse reach 40 kT, while intensity of concurrent electric field achieved values of 10^{14} V/m [17]. According to the predictions of the quantum field theory in such strong electric and magnetic fields which exist close to the bunch boundary, we may expect the occurrence of the Schwinger effect constituting the creation of pairs composed of a particle and antiparticle, e.g.: an electron and positron [18]. The probability of the occurrence of such effects might be subject to separate considerations.

Comparing Fig. 4, 5 with 7, 8 and also 12, 13 with 15, 16, it should be noted that higher values of electric field intensity components occurred in the direction of $0y$ axis than for direction of axis $0z$. It is there from concluded that the beam along $0y$ direction was better focused than in direction of $0z$ and is of smaller size along this direction. Therefore, in accordance with the Gauss law, the appropriate values of components electric field intensity should be bigger for $0z$ direction. Because as part of Lorentz transformation (see formula (18)) the component of electric field intensity in $0y$ direction was connected to magnetic field induction in direction of $0z$ axis (so called “mixing” of components), larger values of component magnetic field induction along $0z$, axis than in direction of axis $0y$ can be observed. It should be added that differences of considered components amount to approximately 22 % and were small in comparison with an over four-fold larger difference of the bunch size in direction of $0y$ and $0z$ axis (see Tab. 3).

References

- [1] F. Ruggiero, *Nominal LHC parameters*, www.lhc-data-exchange.web.cern.ch/lhc-data/exchange/ruggiero.pdf/ (dostęp: 03.02.2015) 7th LTC meeting, 28 May (2003).
- [2] A. I. Wawrzyniak, A. Kisiel, A. Merendziak, P. Borowiec, M. Doruchowski, P. Bulira, Ł. Dudek, P. P. Goryl, K. Karaś, W. Kitka, M. Kopeć, P. Król, M. J. Stankiewicz, K. Wawrzyniak, J. Wilkacz, J. Wiechecki, M. Zajęc, Ł. Żytiniak, C. J. Bocchetta, R. Nietubtyć, *Solaris storage ring commissioning*, Proceedings of IPAC, Korea, Busan 2016, 2895–2897.
- [3] D. Schwartz, D. Berkaev, I. Koop, E. Peredentsev, Yu Rogovsky, Yu. Shatunov, A. Kasaev, A. Kyrpotin, A. Lysenko, V. Prosventov, A. Romanov, A. Senchenko, P. Shatunov, I. Zemlyansky, Yu. Zharinov, *Recent beam-beam effect and at VEPP-2000*, Proceedings of IPAC, Germany, Dresden 2014, 924–927.
- [4] S. Bednarek, J. Płoszajski, *The magnetic and electric field produced by a proton bunch*

from the LHC and project of the chamber for investigations in these fields, Bull. Soc. Sci. Lettres Łódź Sér. Rech. Déform. **67**, no. 1 (2017), 91–106.

- [5] A. V. Feschenko, A. V. Liiou, P. N. Ostroumov, O. Dubois, H. Haseroth, C. Hill, H. Kugler, A. Lombardi, F. Natio, E. Tanke, M. Vretenar, *Study of beam parameters of the proton linac using three dimensional bunch shape monitor*, Proceedings of the International Linear Accelerators Conference (1996), 196–198.
- [6] R. W. Assmann, J. Grbenyuk, *Accelerator physics challenges towards a plasma accelerator with usable beam quality*, Proceedings of IPAC, Germany, Dresden 2014, 961–964.
- [7] R. Brikmann, *Accelerator layout of the XFEL*, Proceedings of the International Linear Accelerators Conference, Germany, Lübeck 2004, 2–6.
- [8] T. Asano, Y. Sakai, K. Inoue, G. Kido, H. Maeda, *Development of Pulsed Magnets at the National Research Institute for Metals*, in: High Magnetic Fields: Application, Generation, Materials, H. J. Schneider-Muntau (Editor) World Scientific, Singapore-New Jersey-London-Hong Kong 1997, 363–370.
- [9] E. M. Purcell, *Electricity and Magnetism, Berkeley Physics Course*, Vol. 2, McGraw-Hill Book Company, New York 1965, 252.
- [10] D. J. Griffiths, *Introduction to Electrodynamics*, Prentice Hall, Inc. Upper Saddle River, New Jersey 1981, 471.
- [11] M. Krupa, L. Soby, *Beam intensity measurements in the Large Hardon Collider*, Proceedings of the 20th International Conference Mixed Design of Integrated Circuits and Systems (2013), 592–597.
- [12] P. Baudrenghien, T. Bohl, T. Linnecar, E. Shaposhnikova, J. Tuckmantel, *Nominal longitudinal parameters for the LHC Beam in the CERN SPS*, Proceedings of the Particle Accelerator Conference, **5** (2003), 3050–3052, DOI: 10.1109/PAC.2003.1289810.
- [13] D. W. Miller, *Online measurements of LHC Beam parameters with the ATLAS High-Level Trigger*, Proceedings of the Real Time Conference (2010), 1–6, DOI: 10.1109/RTC.2010.5750367.
- [14] F. Ruggiero, *Nominal LHC parameters*, www.lhc-data-exchange.web.cern.ch/lhc-data/exchange/rugiero.pdf/ (dostep: 03.02.2015) 7th LTC meeting, 28 May (2003).
- [15] B. E. Kane, A. S. Dzurak, G. R. Facer, R. G. Clark, R. P. Starrett, A. Skougarevsky, N. E. Lumpkin, *Measurement instrumentation for electrical transport experiments in extreme pulsed magnetic fields generated by flux compression*, Review of Scientific Instruments **69**, no. 10 (1997), 3843–3860.
- [16] B. M. Novac, N. D. Hook, R. Smith, *Magnetic flux-compression driven by exploding single-turn coil*, Proceedings of IEEE International Power Modular and High Voltage Conference (2010), 129–132, DOI: 10.1109/IPMHCV.2010.5958311.
- [17] W. Mizerski, *Tablice fizyczno-astrofizyczne*, Wydawnictwo Adamantan, Warszawa 2013, 150, 182.
- [18] H. Stöcker, *Nowoczesne kompendium fizyki*, Wydawnictwo Naukowe PWN, Warszawa 2010, 952.

Chair of Informatics
University of Łódź
Pomorska 149/153, PL-90-236 Łódź
Poland
E-mail: bedastan@uni.lodz.pl
julian-p@wp.pl

Presented by Leszek Wojtczak at the Session of the Mathematical-Physical Commission of the Łódź Society of Sciences and Arts on June 25, 2018.

POLE MAGNETYCZNE WYTWARZANE PRZEZ WIĄZKĘ PROTONÓW O TRÓJWYMIAROWYM ROZKŁADZIE GAUSSA

S t r e s z c z e n i e

Artykuł zawiera opis własnej metody obliczania natężenia pola elektrycznego i indukcji pola magnetycznego, które są wytwarzane przez paczki wchodzące w skład relatywistycznej wiązki protonów. Rozkład przestrzenny gęstości ładunku elektrycznego w tej paczce opisywany jest trójosiowym rozkładem Gaussa. Metoda polega na obliczeniu składowych natężenia pola elektrycznego w układzie poruszającym się wraz z paczką, a następnie zastosowaniu transformacji Lorentza dla pola elektromagnetycznego. W wyniku tego otrzymuje się wartości składowych natężenia pola elektrycznego i indukcji pola magnetycznego w układzie spoczywającym, gdzie mogą być umieszczane próbki badane w tych polach. Wyprowadzone przy użyciu tej metody wzory zostały zebrane w tabelach i przedyskutowane. Wzory te zastosowano do obliczeń na przykładzie paczek protonów, przyspieszanych w akceleratorze LHC. Otrzymane wyniki przedstawiono na wykresach i także przedyskutowano. Użyteczne wartości indukcji pola magnetycznego i natężenia pola elektrycznego są bardzo zbliżone do wartości otrzymanych we wcześniej opublikowanym artykule, w którym zastosowano jednoosiowy rozkład Gaussa. Przedstawione w tym artykule wyniki również potwierdzają możliwość wykorzystania takich paczek cząstek, jako źródła silnych, impulsowych pól magnetycznych, użytecznych m.in. do badań w fizyce ciała stałego, fizyce fazy skondensowanej i elektronice.

Słowa kluczowe: pole magnetyczne, pole elektryczne, rozkład przestrzenny, transformacja Lorentza, wiązka protonów, akcelerator